

Enhanced Macroscopic Quantum Tunneling in $\text{Bi}_2\text{Sr}_2\text{CaCu}_2\text{O}_{8+\delta}$ Intrinsic Josephson-Junction Stacks

X. Y. Jin, J. Lisenfeld, Y. Koval, A. Lukashenko, A. V. Ustinov, and P. Müller

Physikalisches Institut III, Universität Erlangen-Nürnberg, Erwin-Rommel-Strasse 1, D-91058 Erlangen, Germany

(Received 22 December 2005; published 3 May 2006)

We have investigated macroscopic quantum tunneling in $\text{Bi}_2\text{Sr}_2\text{CaCu}_2\text{O}_{8+\delta}$ intrinsic Josephson junctions at millikelvin temperatures using microwave irradiation. Measurements show that the escape rate for uniformly switching stacks of N junctions is about N^2 times higher than that of a single junction having the same plasma frequency. We argue that this gigantic enhancement of the macroscopic quantum tunneling rate in stacks is boosted by current fluctuations which occur in the series array of junctions loaded by the impedance of the environment.

DOI: [10.1103/PhysRevLett.96.177003](https://doi.org/10.1103/PhysRevLett.96.177003)

PACS numbers: 74.72.Hs, 73.23.-b, 74.50.+r, 85.25.Cp

Twenty years since its discovery, macroscopic quantum tunneling (MQT) in Josephson junctions remains a fascinating phenomenon which attracts the interest of a broad physics community. MQT was first observed in Nb Josephson junctions at very low temperatures [1] and has been used to study energy level quantization by microwave absorption [2]. More recently, the so-called phase qubits based on MQT in current-biased Josephson junctions have been reported as very promising hardware for quantum information processing [3–5].

Because of their d -wave order parameter symmetry [6,7], cuprate high- T_c superconductors were initially regarded unsuitable for MQT experiments. However, it has been argued that although there are nodes in the d -wave order parameter, MQT should not be suppressed completely in high- T_c Josephson junctions [7,8]. Meanwhile, recent measurements on $\text{YBa}_2\text{Cu}_3\text{O}_{7-\delta}$ grain boundary junctions show the solid evidence of MQT [9].

On the other hand, intrinsic Josephson junctions (IJJs) in layered high- T_c superconductors [10,11] are rather attractive candidates for MQT experiments. IJJs in $\text{Bi}_2\text{Sr}_2\text{CaCu}_2\text{O}_{8+\delta}$ (BSCCO) are formed by pairs of CuO_2 double planes, separated by a Bi_2O_3 insulating layer. They have a much higher Josephson coupling energy than grain boundary junctions and a better homogeneity, as they are located inside a more or less perfect single crystal. Moreover, intrinsic junctions exhibit current transport along the c -axis direction, i.e., perpendicular to the copper oxide layers, where the nodes of the $d_{x^2-y^2}$ order parameter should not affect MQT at all. With the recent invention of a double-sided fabrication technique [12], one can avoid heating the junctions by contact resistance. This makes MQT in IJJs practically attainable. Recently, MQT has been observed on a single junction in $\text{Bi}_2\text{Sr}_2\text{CaCu}_2\text{O}_{8+\delta}$ IJJs [13,14]. The temperature T^* of the crossover between thermal and quantum escape was reported to be rather high.

In this Letter, we present an experimental study of MQT in IJJs using microwave spectroscopy. We demonstrate that the unique uniform array structure of intrinsic Josephson junction stacks causes an enormous enhancement of the

tunneling rate. We argue that this enhancement can be caused by current fluctuations in the stack.

The samples were fabricated using the standard double-sided ion beam etching technique [12]. The stack height ranges from approximately 7.5 to 15 nm; i.e., the number of junctions N in our IJJ series arrays is between 50 and 100. The junction area varied for different stacks from 1×2 to $2 \times 3 \mu\text{m}^2$. Critical current densities j_c were between 0.7–2.8 kA/cm². Sample parameters are summarized in Table I. Current-voltage (I - V) characteristics were measured with a standard four-terminal configuration using current biasing. Experiments were performed in a ³He cryostat with a minimum temperature of 300 mK and in a ³He/⁴He dilution refrigerator with a base temperature of 10 mK.

We investigated two different types of samples. Their typical I - V characteristics are presented in Fig. 1. In the first case, at least one junction had a critical current significantly lower than those of the rest of the stack. This was achieved either by exposing the unprotected side of the crystal to ambient atmosphere, resulting in a reduced critical current density, or by overetching resulting in a reduced cross-sectional area. When increasing the current, we observed voltage jumps from one branch to the next in steps of approximately 25 mV [Fig. 1(a)]. Because of the large difference of the critical current, it is always the same junction that switches to its resistive state first. We call this behavior “single-junction switching” and denote this

TABLE I. Sample parameters measured.

#	size (μm^2)	I_s (μA)	T^* (mK)	f_p^0 (GHz)	γ_s (%)	N
SJ1	2×3	57.7	300	120	99.0	1
SJ2	2×3	162.5	450	180	99.2	1
SJ3	2×3	67.4	320	135	98.9	1
US1	1×3	38.2	700	138	96.5	46
US2	2×2	31.0	500	126	96.3	42
US3	2×3	57.2	550	140	97.2	50
US4	2×3	65.5	620	150	97.3	~100

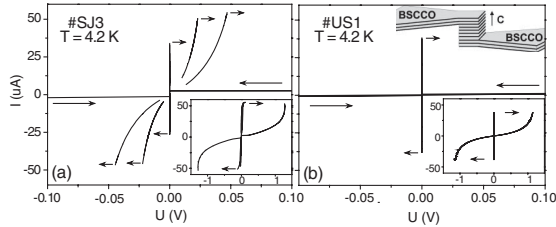


FIG. 1. I - V characteristics: (a) One-by-one switching of three junctions in a stack, #SJ3; (b) uniform switching of the whole stack, #US1. The insets show the full-range I - V curves for both samples. The sample geometry is sketched in the upper right corner.

type of samples as the #SJ series. In the second case, the stack is so homogeneous that upon *increasing* the current, we never observed any stable states between zero voltage and 1.14 V, where all junctions are in the resistive state [Fig. 1(b)]. We call that behavior “uniform-stack switching” and denote this type of samples as the #US series. Nevertheless, we find that many branches corresponding to different numbers of resistive junctions are still there. They can be easily traced up from the return curve of the resistive state [10–12].

Distributions of the switching current, I_s , at which the junctions escape from the zero-voltage state [15] were measured using a high-resolution ramp-time based setup [16]. The bias current was ramped up with a rate of 200 mA/s. After detecting a switching event by a voltage threshold of 20 μ V, the current was switched to zero within less than 10 μ s in order to avoid heating effects. Monitoring the voltage on a fast oscilloscope for #US-type samples showed that the current decrease was fast enough so that any stack always switched to its first resistive branch, i.e., to a state with one resistive junction. Based on this fact we emphasize that regarding dissipation, both types of samples were measured under *exactly* the same experimental conditions. Switching current distributions were measured at temperatures between 20 mK and 12 K using a repetition rate of 600 Hz. The switching current statistics was determined from 20 000 to 60 000 switching events. The switching probability $P(I)$ shown in the inset of Fig. 2 is defined as the number of switching events per μ A normalized to the total number of events. The standard deviation σ of the switching current was determined from the width of the $P(I)$ curve. Figure 2 shows σ as a function of temperature for samples #SJ1 and #US1. The saturation of $\sigma(T)$ at low temperatures corresponds to a crossover from thermal activation to MQT. For sample #SJ1 the saturation is not complete in Fig. 2. This is due to the fact that this experiment was done in a ^3He cryostat where the lowest temperature was 300 mK. We verified complete saturation in our experiments in the dilution refrigerator. Nevertheless, one may still see in Fig. 2 that the crossover temperature T^* of the single-junction sample #SJ1 is about 300 mK, while the uniform-switching sample #US1 shows

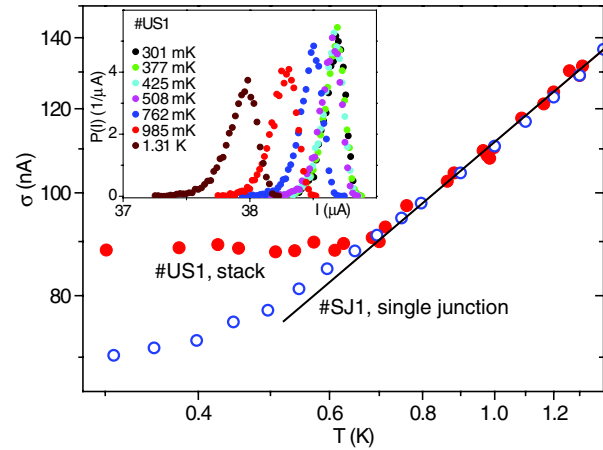


FIG. 2 (color online). Temperature dependence of the standard deviation of the switching current from the zero-voltage state. Solid circles: sample #US1; open circles: sample #SJ1. The straight line is a linear fit to all data points above 700 mK. The inset shows switching current distributions for #US1. For better comparison, the #US1 data were divided by a factor of 1.09.

T^* of about 700 mK. This discrepancy cannot be fully accounted by the difference in the critical currents.

At temperatures below T^* , we measured the switching current distributions under microwave radiation in the frequency range between 10 and 40 GHz. Such measurements allow us to determine the plasma frequency ω_p^0 and the absolute value of the fluctuation-free critical current I_c directly [2]. Here, microwave spectroscopy serves as a tool to determine the energy level separation in the quantum regime. It should be noticed that quantum transitions between levels cannot be easily distinguished from classical plasma resonance peaks using just spectroscopy data [17]. However, below the crossover temperature T^* quantum fluctuations dominate thermal ones and quantum mechanics is appropriate for describing the system. Since the zero-bias plasma frequency $f_p^0 = \omega_p^0/2\pi$ for the samples was well above 100 GHz, we used multiphoton [18] rather than single-photon absorption in our measurements.

As the microwave power is increased, the $P(I)$ distribution becomes double peaked. The microwave-induced peak at lower currents corresponds to a plasma resonance in the junction. In the quantum picture, this peak is interpreted as tunneling from highly populated energy level(s). Figure 3(a) shows a density plot of the switching current distribution of a uniform-switching stack versus microwave power at 38.2 GHz. Figure 3(b) shows the corresponding enhancement of the escape rate. The deviation of the Lorentzian at lower bias is primarily due to the smaller number of counts. The double-peaked $P(I)$ distribution develops at a microwave power of about -1 dBm referred to the top of the cryostat. The two-photon resonance current peak appears at about 57.0 μ A. It should be noted that the width of the resonance peak is smaller than the distribution width at zero microwave power, which indicates

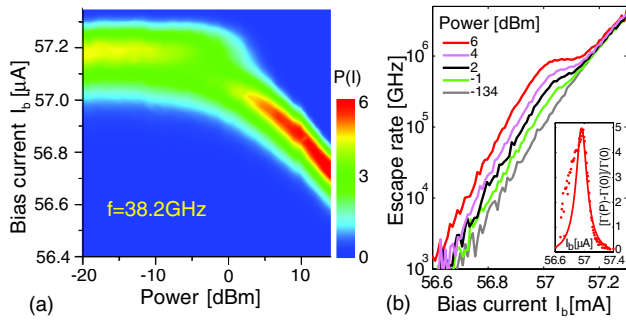


FIG. 3 (color online). (a) Density plot of switching current vs microwave power for two-photon absorption in sample #US3 at 30 mK. The switching probability $P(I)$ is color coded according to the bar on the right-hand side. (b) The corresponding enhancement of the escape rate at different microwave powers. The inset shows the fit of the 6 dBm enhancement curve with a Lorentzian.

that the standard deviation of $P(I)$ measured without microwaves is not limited by current noise in our setup. The resonance current I_r is defined as the position of the resonant peak when both peaks have equal amplitudes. The results at different microwave frequencies are summarized in Fig. 4. The data are fitted to [2]

$$\omega_p = \frac{1}{n} \omega_p^0 (1 - \gamma^2)^{1/4}, \quad (1)$$

where ω_p is the plasma frequency of the junction at the normalized bias current γ , ω_p^0 is the plasma frequency at zero bias, and n is the number of photons taking part in the absorption process. $\gamma = I_b/I_c$ is given in normalized units, where I_b is the bias current and I_c is the fitted fluctuation-free critical current. The data in Fig. 4 show the best fit to Eq. (1) by assuming two- and three-photon absorption. At lower frequencies and high powers we observed multiphoton peaks up to $n = 6$ (not shown). From the fits we obtain $f_p^0 = \omega_p^0/2\pi = 150$ GHz (sample #US3), and $f_p^0 = 180$ GHz (sample #SJ2). The fitted f_p^0 of the other samples are shown in Table I. The obtained plasma frequencies provide an estimate for the junction capacitance per unit area $C = j_c/(2\pi\Phi_0 f_p^0)$, where Φ_0 is the magnetic flux quantum. Our measurements yield $C = 3.9 \mu\text{F}/\text{cm}^2$ and $\epsilon_r = 5.3$, which conforms well with the value of $\epsilon_r = 5$ obtained in earlier work [19].

From the results shown in Fig. 4 and Table I, one may notice that the normalized switching current $\gamma_s = I_s/I_c$ of the uniformly switching stacks is significantly lower than that of the single-junction switching samples. The typical value of γ_s for single-junction samples is about 99% of the fluctuation-free critical current I_c , whereas for the uniform-switching stacks it is only 96%. The switching range of the single-junction samples is fairly similar to that of Nb junctions with comparable critical current densities, where γ_s is also close to 99% [18]. On the contrary, the normalized switching bias current γ_s of uniformly switching stack samples is about 3% smaller. This discrepancy

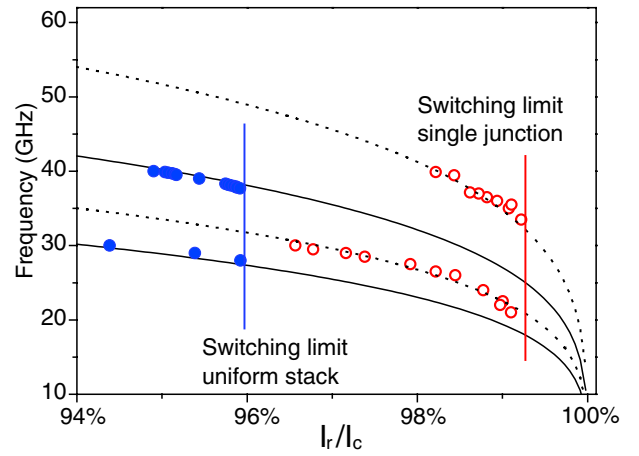


FIG. 4 (color online). Applied microwave frequency versus normalized resonance current for sample #SJ2 (open circles) and #US3 (solid circles) measured at 20 mK. The data are fitted to Eq. (1) using $n = 2$ (upper dotted line and upper solid line) and $n = 3$ (lower lines). The vertical lines mark the maximum switching current of the samples.

can explain the difference in T^* for #SJ and #US samples. The plasma frequency ω_p^s at the switching current is given by Eq. (1) with $\gamma = \gamma_s$. For a single junction, the temperature of the crossover from thermally activated escape to MQT is expected [20] to be $T^* \approx \hbar\omega_p^s/2\pi k_B$. For uniformly switching samples, the premature switching at lower γ_s leads to the high ω_p^s and thus to an enhanced T^* .

In the quantum regime, a single Josephson junction escapes through the energy barrier with an escape rate Γ determined by [21]

$$\Gamma = \frac{\omega_p}{2\pi} \left(\frac{864 U_0 \pi}{\hbar \omega_p} \right)^{1/2} \exp\left(-\frac{36}{5} \frac{U_0}{\hbar \omega_p} \right), \quad (2)$$

where ω_p is given by Eq. (1), $U_0 = E_J \frac{4\sqrt{2}}{3} (1 - \gamma)^{3/2}$ is the height of the potential barrier at $\gamma \leq 1$, and $E_J = \Phi_0 I_c / 2\pi$ is the Josephson coupling energy. In Fig. 5 we plot Eq. (2) using the values of ω_p^0 and I_c in Table I for samples #US1, #US4, and #SJ3, respectively (solid lines). The interconnected dots were determined from the measured $P(I)$ histograms. For single-junction sample #SJ3, one can see that experiment agrees well with the theory. However, there is a huge difference between theory and experiment for both uniformly switching samples.

We used the mean switching bias γ_s of each sample to mark the intersection of γ_s with the theoretical curves in Fig. 5 by large open dots. According to the theory, these dots should correspond to the most probable escape current. One can see that the intersections of γ_s with the experimental curves show actual escape rates higher by a factor of roughly 2000 (#US1) and 10 000 (#US4). This difference is marked by the vertical arrows in Fig. 5. Samples listed in Table I have different sizes and j_c 's. We have measured them in different setups and at different

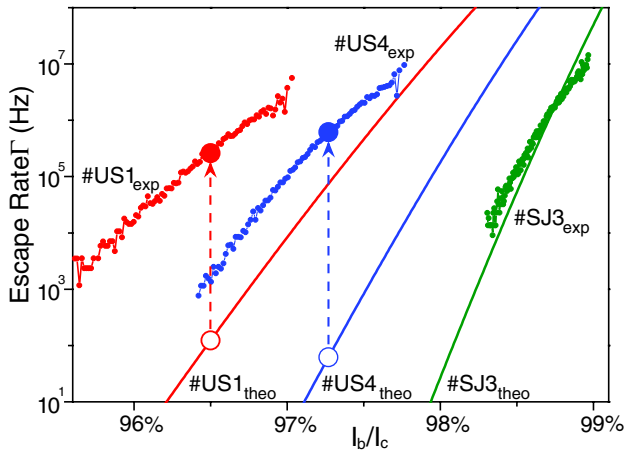


FIG. 5 (color online). Escape rate versus bias current for uniformly switching stack samples #US1 and #US4 and single-junction switching sample #SJ3. The solid lines are calculated by the single-junction quantum escape theory (2). The points interconnected by lines are extracted from the measured $P(I)$ distributions. The vertical arrows indicate the enhancement of the escape rate (see text).

temperatures. Experiments for *all* single-junction samples well agree with theory (2). On the other hand, for *all* uniformly switching samples we always found a huge difference between the measured data and single-junction model given by Eq. (2). We therefore conclude that the single-junction tunneling theory is not applicable to the uniform-switching stacks.

The value of N in #US samples can be determined by counting the number of resistive branches in the I - V characteristics. Assuming that the single-junction escape rate is enhanced by a factor of N^2 , one can renormalize the peak escape rate of all #US samples. In Fig. 5 we have chosen to show samples #US1 with $N = 46$ and #US4 with $N = 100$. We find that the N^2 corrected values shown by large solid dots conform pretty well to the experimental data. Moreover, our data for samples #US2 and #US3 (see Table I) also match this N^2 correction.

If there would be no interaction between N identical junctions in a current-biased series array, the escape rate Γ (the probability that at least one junction switches at a given bias current) should be merely enhanced by a factor N with respect to a single junction. If we assume that switching of any junction in the array is triggered, in addition to its own fluctuations, by its nearest neighbors in the array (e.g., via charge coupling through the shared CuO_2 double-planes), then we should get an enhancement by a factor of about $3N$. However, experiments imply that the enhancement of the escape rate in stacks is proportional to N^2 . This is possible when there is an interaction between *any pair* out of the N junctions. Such interaction occurs when the stack of junctions connected in series is loaded in parallel by a relatively low impedance. Fluctuations of the phase difference of a single junction change its parametric

Josephson inductance and thus the total inductance of the array. The external bias current is split up between the array and the external impedance, which can be regarded as the impedance of the environment at the plasma frequency. The bias current flowing through the array thus changes under fluctuations in any junction. A specific analysis of this model goes beyond the scope of this experimental Letter.

In conclusion, we have found a drastically enhanced escape rate of macroscopic quantum tunneling in uniformly switching $\text{Bi}_2\text{Sr}_2\text{CaCu}_2\text{O}_{8+\delta}$ intrinsic Josephson junction stacks. This enhancement adds a factor of approximately N^2 to the quantum escape rate of a single Josephson junction. This can be caused by large quantum fluctuations due to interactions among the N junctions and results in a significant increase of the crossover temperature T^* between the thermal activation regime and quantum tunneling.

We thank Dr. H. B. Wang for providing high quality $\text{Bi}_2\text{Sr}_2\text{CaCu}_2\text{O}_{8+\delta}$ crystals and for helpful discussions. This work was supported by Deutsche Forschungsgemeinschaft.

-
- [1] R. F. Voss and R. A. Webb, Phys. Rev. Lett. **47**, 265 (1981); M. H. Devoret, J. M. Martinis, and J. Clarke, Phys. Rev. Lett. **55**, 1908 (1985).
 - [2] J. M. Martinis, M. H. Devoret, and J. Clarke, Phys. Rev. Lett. **55**, 1543 (1985); J. M. Martinis, M. H. Devoret, and J. Clarke, Phys. Rev. B **35**, 4682 (1987); J. Clarke *et al.*, Science **239**, 992 (1988).
 - [3] J. M. Martinis *et al.*, Phys. Rev. Lett. **89**, 117901 (2002).
 - [4] A. J. Berkley *et al.*, Science **300**, 1548 (2003).
 - [5] R. McDermott *et al.*, Science **307**, 1299 (2005).
 - [6] C. C. Tsuei and J. R. Kirtley, Rev. Mod. Phys. **72**, 969 (2000).
 - [7] M. H. S. Amin and A. Y. Smirnov, Phys. Rev. Lett. **92**, 017001 (2004); Y. V. Fominov, A. A. Golubov, and M. Y. Kupriyanov, JETP Lett. **77**, 587 (2003).
 - [8] S. Kawabata *et al.*, Phys. Rev. B **70**, 132505 (2004).
 - [9] T. Bauch *et al.*, Science **311**, 57 (2006); T. Bauch *et al.*, Phys. Rev. Lett. **94**, 087003 (2005).
 - [10] R. Kleiner *et al.*, Phys. Rev. Lett. **68**, 2394 (1992).
 - [11] R. Kleiner and P. Müller, Phys. Rev. B **49**, 1327 (1994).
 - [12] H. B. Wang *et al.*, Appl. Phys. Lett. **78**, 4010 (2001).
 - [13] K. Inomata *et al.*, Phys. Rev. Lett. **95**, 107005 (2005).
 - [14] H. B. Wang (personal communication).
 - [15] T. Fulton and L. Dunkleberger, Phys. Rev. B **9**, 4760 (1974).
 - [16] A. Wallraff *et al.*, Rev. Sci. Instrum. **74**, 3740 (2003).
 - [17] N. Grønbech-Jensen *et al.*, Phys. Rev. Lett. **93**, 107002 (2004).
 - [18] A. Wallraff *et al.*, Phys. Rev. Lett. **90**, 037003 (2003).
 - [19] W. Walkenhorst *et al.*, Phys. Rev. B **56**, 8396 (1997).
 - [20] H. Grabert *et al.*, Phys. Rev. B **36**, 1931 (1987).
 - [21] A. O. Caldeira and A. J. Leggett, Phys. Rev. Lett. **46**, 211 (1981).